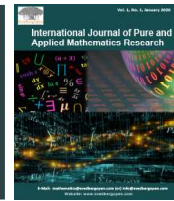




International Journal of Pure and Applied Mathematics Research

Publisher's Home Page: <https://www.svedbergopen.com/>



Research Paper

Open Access

Mathematical Modeling of Dynamics of Cancer Invasion in Human Body Tissues

Mogire Dinnah Kemunto^{1*}, Kerongo Joash² and Vincent Bulinda³

¹Department of Mathematics and Actuarial Science, Kisii University, Kenya. E-mail: dinnahkemuntomogire@gmail.com

²Department of Mathematics and Actuarial Science, Kisii University, Kenya. E-mail: jkerongo@kisiiversity.ac.ke

³Department of Mathematics and Actuarial Science, Kisii University, Kenya. E-mail: bulinda@kisiiversity.ac.ke

Article Info

Volume 3, Issue 1, April 2023

Received : 13 October 2022

Accepted : 19 March 2023

Published : 05 April 2023

doi: [10.51483/IJPAMR.3.1.2023.52-69](https://doi.org/10.51483/IJPAMR.3.1.2023.52-69)

Abstract

The dynamics of invasion of cancer cells into the human body tissues and metastasis are the main causes of death in patients with cancer. This study deals with theoretical investigation of the dynamics of invasion of cancer cells for tumour growths in human body tissues using discretized Cahn-Hilliard, concentration and reaction-diffusion equations which were solved by Finite Difference Method with the aid of MATLAB computer software. A Crank-Nicolson numerical scheme was developed for the discretized model equations. The numerical result obtained was used to describe the dynamics of cancer invasion of tissues with respect to cancer cells density on tumour growth, turbulence and mobility, and the equilibrium between charge and discharge of cancer cells. The results of the study provide new insights into combating cancer disease by providing mitigating and intervention measures to this major health problem.

Keywords: *Cancer cells, Finite Difference Method, Tumor growth*

© 2023 Mogire Dinnah Kemunto et al. This is an open access article under the CC BY license (<https://creativecommons.org/licenses/by/4.0/>), which permits unrestricted use, distribution, and reproduction in any medium, provided you give appropriate credit to the original author(s) and the source, provide a link to the Creative Commons license, and indicate if changes were made.

1. Introduction

Cancer remains the world's primary cause of death, despite continuous therapeutic advances, making it a major public health issue with devastating societal consequences. From what can be gleaned from the databases of the World Health Organization (WHO) and the United Nations (UN), it is clear that cancer is currently, and is likely to remain, one of the top causes of mortality around the world. Cancer ranks high on the list of global killers and causes a great deal of suffering. Annually, it's responsible for the deaths of around six million individuals. In light of this, it is clear why efforts toward cancer prevention, treatment, and discovery are so vital. The anticipated 18.1 million new cases and 9.6 million deaths from cancer worldwide in 2018 demonstrate the continued escalation in this disease's global burden. It's putting a major burden on healthcare systems and populations worldwide. WHO's Global Cancer Observatory projects that ten million people will lose their lives to cancer in 2020, up from nine million in 2018, and that number will climb to over sixteen and a half million by 2040 if preventative measures aren't implemented (Roose et al., 2007).

* Corresponding author: Mogire Dinnah Kemunto, Department of Mathematics and Actuarial Science, Kisii University, Kenya. E-mail: dinnahkemuntomogire@gmail.com

2789-9160/© 2023. Mogire Dinnah Kemunto et al. This is an open access article distributed under the Creative Commons Attribution License, which permits unrestricted use, distribution, and reproduction in any medium, provided the original work is properly cited.

Some of the biggest obstacles to a comprehensive understanding of cancer development and treatment are metastatic colonization, dormancy, relapse, multiple drug therapy, immune resistance, and the use of mathematical models and simulations to predict the course of the disease and the optimal treatment. What makes this phenomenon so difficult to understand is that cancer is an ancient disease that appears to be inherent to the complexity of creatures produced by evolution, in contrast to viral infections, which only became major killers with the rise of vast societies a few hundred years ago (Perthame, 2016; Brassel and Bretin, 2011).

Cancer is a disease characterized by a series of evolutionary steps at the somatic level, including tumor initiation, development, dissemination, immune evasion, and the emergence and maintenance of drug resistance. The evolutionary history of a tumor can be deduced from molecular data, and evolutionary theory can be used to examine the dynamics of tumor cell populations. The promise of several approaches to modeling cancer's development has been recently assessed. They include the phylogenetic approaches to modeling the evolutionary relationship between tumor subclones and the probabilistic graphical models for characterizing dependencies among mutations, as well as models of tumor onset and progression based on the dynamics of the population. Understanding the genesis of tumors, as well as the likely course of a disease and the effectiveness of treatments like targeted therapy, can be greatly aided by evolutionary modeling. Hence, the multistep theory is incorporated into the population dynamics models. Tumor phylogenetic tree, single-cell approach, hybrid models, and stochastic models are some of the phylogenetic approaches (Beerenwinkel et al., 2015).

In order to deal with the difficulties associated with Tumor growth, Perthame (2016) provides some invasion models. First, there are models of interplanetary invasion based on the Reaction-Diffusion Equations. Considered alongside constrained expansion and dispersal via diffusion, it depicts the spread of an infectious disease, the arrival of a new species (with no natural enemies), a combustion wave, or a new way of thinking. Second, the Fisher-KPP model is suggested to model the spatiotemporal development of a Tumor under chemotherapeutic influence.

In order to tackle the many difficulties associated with Tumor development, several models based on Ordinary Differential Equations (ODEs) have been presented. Two species, one predator and one prey, interacting in a biological system is the focus of several theoretical frameworks, such as the Lotka-Volterra model. cells that are both active and dormant, or P-Q, Model; According to the NCI's Dictionary of Cancer Terminology, cell proliferation refers to the increase in cell population that occurs as a result of normal cellular processes including growth and division. An absence of proliferation that is both transitory and reversible characterizes a state called quiescence. To wit. When it comes to describing and analyzing the immune response to cancer growth, the ODEs models are invaluable tools (Fornier et al., 2011).

Tumor growth models have been demonstrated to be an essential tool in the development of an engineering foundation for cancer therapy through the use of therapeutic procedure design coupled with control engineering or the use of the models for simulation and assessment of treatment processes. This work further demonstrates the usefulness of mathematical modeling in describing Tumor formation, a process of great complexity, by highlighting the characteristics and physiological processes of the Tumors. For this reason, they built a partial differential equation-based mathematical model for Tumor growth and presented its results in their study. In this model, the densities of proliferative, quiescent, necrotic, and surrounding cells are described together with the flow of nutrients using a deterministic model of an avascular Tumor growth framed in a system of nonlinear coupled PDEs (Akhtar et al., 2021).

The final model equation of this study was solved numerically in two dimensions. With the help of the finite difference approximations, spatial discretization was conducted on the model equations, reducing them to a set of time-dependent partial differential equations that were solved with the help of the central difference formulas.

This paper is organized as follows. First, the background to the study is described in section 1. Then, the governing mathematical principles and equations are given in Section 2, model conceptualization and applications are presented in Section 3, results and discussion on results is provided in Section 4, summary and conclusion in Section 5, and recommendations in Section 6.

2. Background

The mechanisms involved in the evolution of cancer are extremely intricate and dynamic. Due to its enormous complexity, cancer has become a very effective human killer in modern times by hindering early identification and treatment. The numerous methods and approaches used to treat cancer aim to stop the disease's spread at different phases (such as

immortalization or unending cell development, transformation, and metastasis). Yet, the bigger achievements in science and medicine have not yet connected all the dots, leaving us without an apparent solution at this time. We are still unable to develop a vaccine or an effective anti-cancer medicine since we still don't fully understand how cancer develops and manifests (Fornier and Sagot, 2011).

One such area that pertains to the cutting-edge study of cancer growth and treatment is mathematical modeling. The goal of developing mathematical models of cancer is to forecast Tumor growth and treatment options. A highly associative topic, mathematical modeling integrates the real-world issue with multiple simulative models built using mathematical techniques.

There is still tremendous space for improvement in cancer therapy, despite the fact that it has been more effective for many Tumors in recent years. Knowing the basics of how Tumor cells invade can help doctors prescribe treatments and preventative measures for cancer. This cancer invasion process can be mathematically described as a system (or systems) of differential equations, which, when solved, will essentially offer a useful contribution to solving the cancer problem. In order to maximize the cancer problem, mathematical oncology will be employed to deliver an integrated solution without the need for clinical trials and experimentation. Therefore, there will be need to determine integrable theoretical solution to the dynamics of cancer invasion in reference to density of Tumor cells, turbulence and motility of Tumor cells and to determine the equilibrium between charge and discharge of Tumor cells (Socolofsky and Jirka, 2002; Xuelian et al., 2019).

2.1. Governing Equations and Theories

The section discusses the equations that govern the growth rate, concentration and invasion of cancer cells with reference to its density, growth rate, degradation, renewal, mobility and concentration in the Tumor. Since this is a two-dimensional problem, the equations are presented along the horizontal and vertical axes. The following universal laws form the basis for the general equations in the dynamics of cancer cells: The equations of diffusion and concentration, as well as the Cahn-Hilliard equation. In order to facilitate their incorporation into the aforementioned computer code, these essential equations are presented in Cartesian form.

It is not possible to get analytical solutions to the equations driving cancer invasion and Tumor growth since they are extremely non-linear PDEs. The Navier-Stokes equations (named after their discoverers Claude-Louis Navier and George Gabriel Stokes) are used to characterize the dynamics of fluids. These equations are important to the fields of economics and academia. The Navier-Stokes equations are used to model the flow of fluids, such as the weather, ocean currents, water flow in a pipe, and air flow over a wing. Its use as models extends to other fields, such as the analysis of pollutants, the development of power plants, and the research of blood flow. These equations include the following;

2.1.1. Continuity Equation

The continuity equation in 3-D is given as:

$$\frac{\partial u}{\partial x} + \frac{\partial v}{\partial y} + \frac{\partial w}{\partial z} = 0 \quad \dots(2.1)$$

Along with a mathematical definition of the relevant process, the equation for conservation of mass (or continuity equation) can be used to derive a differential equation describing the movement of cancer cells. The conservation Equation (2.1) can be examined under two distinct circumstances. The first scenario is satisfied when the charging and discharging rates of the cancer cells are equal. The second scenario involves investigating what occurs when the charging and discharging rates of cancer cells are different. The first condition will be considered in this study.

2.1.2. Momentum Equation

According to the law of conservation of momentum, also known as the principle of momentum conservation in fluid dynamics, the momentum of a closed system does not change. The momentum equation, a form of Newton's Second Law, describes the relationship between the total force acting on an element and the rate of change in that element's momentum or acceleration. These Partial Differential Equations (PDEs) provide the incompressible version of the Navier-Stokes equations. The Navier-Stokes equation in x -direction is given as:

$$\rho \left(\frac{\partial u}{\partial t} + u \frac{\partial u}{\partial x} + v \frac{\partial u}{\partial y} \right) = -\frac{\partial p}{\partial x} + \mu \left(\frac{\partial^2 u}{\partial x^2} + \frac{\partial^2 u}{\partial y^2} \right) + \rho f \quad \dots(2.2)$$

while the in y-direction Navier-Stokes equation takes the form

$$\rho \left(\frac{\partial v}{\partial t} + v \frac{\partial v}{\partial x} + v \frac{\partial v}{\partial y} \right) = -\frac{\partial p}{\partial y} + \mu \left(\frac{\partial^2 v}{\partial x^2} + \frac{\partial^2 v}{\partial y^2} \right) + \rho f \quad \dots(2.3)$$

2.1.3. Concentration Equation

In fluid mechanics, the concentration equation (derived from the scalar transport equation) describes how material is transported (and, thus, mixed) from a continuum viewpoint. In this equation, material (with concentration C) is passively carried by a velocity field u while simultaneously undergoing diffusion (where D is the diffusion coefficient). In contrast to the Navier-Stokes equations, the velocity field u is known, and with the given initial condition, the evolution of the concentration can be determined for all time. The application of the concentration equation to physical systems can shed light onto how these systems diffuse for different parameters.

The net movement of the cancer cells in x and y respectively are

$$\begin{aligned} u \delta x + \delta x \\ u \delta y + \delta y \end{aligned} \quad \dots(2.4)$$

The total flux in the x and y directions are J_x and J_y , respectively. Including the advective transport and a Fickian diffusion term to Equation (2.4) gives

$$J_x = uC + C_x = uC - D \frac{\partial C}{\partial x} \quad \dots(2.5)$$

$$J_y = vC + C_y = vC - D \frac{\partial C}{\partial y} \quad \dots(2.6)$$

$$\frac{\partial C}{\partial t} + u \frac{\partial C}{\partial x} + v \frac{\partial C}{\partial y} = D \left(\frac{\partial^2 C}{\partial x^2} + \frac{\partial^2 C}{\partial y^2} \right) \quad \dots(2.7)$$

where $u(x, y, t)$ is the given divergence-free advective velocity vector field, t is time and $C_{(x,y,t)}$ is the fluid concentration levels in mixing process, $C(x, y, t)$ is the concentration of cancer cells and D is the diffusion coefficient.

2.1.4. Energy Equation

Energy can neither be created nor be destroyed; can only change physical form. Energy equation can be written in many different ways, such as the one given below:

$$\rho C_p \left(\frac{\partial \theta}{\partial t} + u \frac{\partial \theta}{\partial x} + v \frac{\partial \theta}{\partial y} \right) = \kappa \nabla^2 \theta + \mu \phi \quad \dots(2.8)$$

2.1.5. Cahn-Hilliard Equation

The original governing equations for the tumor growth in Wise *et al* (2008), are the Cahn-Hilliard equation

$$\frac{\partial \phi}{\partial t} = M \rho \left(\frac{\partial^2 \phi}{\partial x^2} + \frac{\partial^2 \phi}{\partial y^2} + \frac{\partial^2 \phi}{\partial z^2} \right) = -v \left(\frac{\partial \phi}{\partial x} + \frac{\partial \phi}{\partial y} + \frac{\partial \phi}{\partial z} \right) + S_1 \phi \quad \dots(2.9)$$

$$\mu = (F'(\phi) - \varepsilon^2 \Delta \phi) \quad \dots(2.10)$$

$$\mu = \nabla P - \frac{\gamma}{\varepsilon} \phi \nabla \mu \quad \dots(2.11)$$

where, mobility $M > 0$.

The diffuse interface model of Wise *et al.* (2008) is reformulated using the conservative second-order AC equation with a space-time dependent Lagrange multiplier in Equation (2.11).

The diffuse interface model of Wise *et al.* (2008), involves the second-order CH equation with a source term. The proposed model consists of the following three equations:

$$\frac{\partial \phi}{\partial t} = M \rho \left(\frac{\partial^2 \phi}{\partial x^2} + \frac{\partial^2 \phi}{\partial y^2} + \frac{\partial^2 \phi}{\partial z^2} \right) = -v \left(\frac{\partial \phi}{\partial x} + \frac{\partial \phi}{\partial y} + \frac{\partial \phi}{\partial z} \right) + S_r \phi \quad \dots(2.12)$$

$$\frac{\partial \psi}{\partial t} = M \mu \left(\frac{\partial^2 \psi}{\partial x^2} + \frac{\partial^2 \psi}{\partial y^2} \right) - u \left(\frac{\partial \psi}{\partial x} + \frac{\partial \psi}{\partial y} \right) + \phi S_D \quad \dots(2.13)$$

$$\frac{\partial \phi}{\partial t} = M \phi \left(-F'(\phi) + c^2 \left(\frac{\partial \phi}{\partial x} + \frac{\partial \phi}{\partial y} \right) \beta(t) F(\phi) \right) \quad \dots(2.14)$$

3. Model Conceptualization

Figure 1 below demonstrates the flow of cancer cells in the cylindrical arterial section. x is the horizontal coordinate and y is the vertical coordinate. The flowing layer depth is δ , and the length of the tissue under consideration is L .

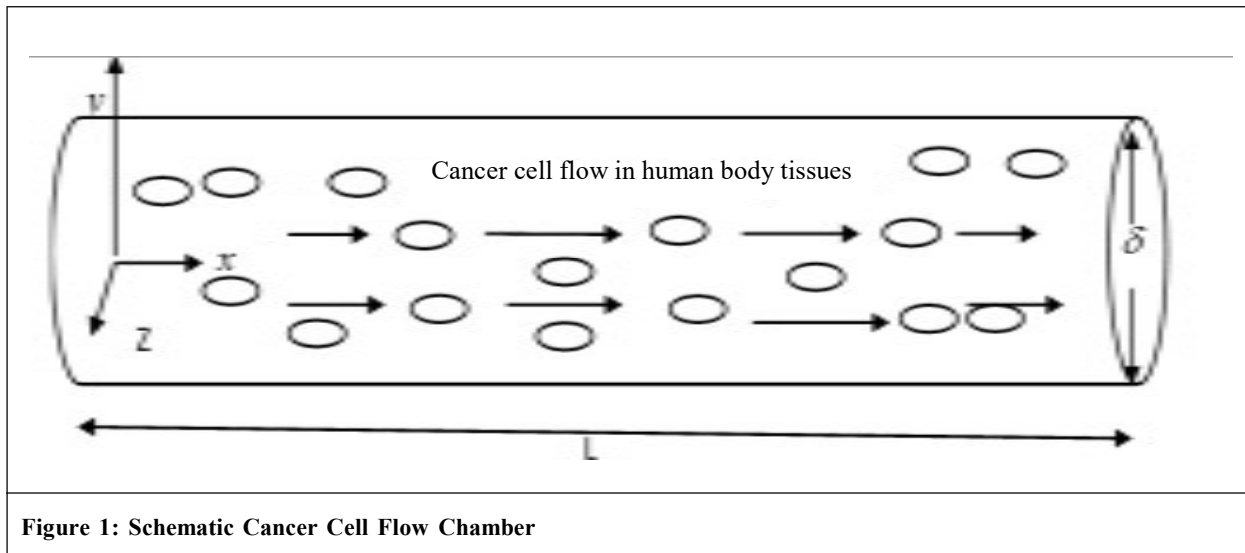


Figure 1: Schematic Cancer Cell Flow Chamber

Cancer cells, which are seen as small, circular particles, and blood, which is depicted as the fluid represented by the arrow, enter the cylinder-shaped flow chamber and become well mixed. A current of fluid is moving through the chamber. Arteries, veins, and capillaries are the blood vessels (tubes) via which blood travels throughout the body. This demonstrates the functioning process of the cardiovascular system. The system is used to transport gases such as oxygen and carbon dioxide. The presence of blood supply is crucial in the metastatic process. Some cancer cells are able to leave the main Tumor and enter the bloodstream by squeezing through tiny crevices in the walls of blood vessels. Modern cancer cells in the circulation are able to adhere to the walls of blood vessels, creating microscopic channels through which they can inject genetic information that changes the endothelial cells lining the blood vessels, making them far more friendly to other cancer cells (Katira *et al.*, 2013).

In nature, transport occurs in fluids through the combination of advection and diffusion (Sharif and Wellstein, 2015). It is therefore necessary to mathematically incorporate advection equation into concentration equation.

The concentration equation is derived using the principle of superposition, which states that linearly independent processes such as advection and diffusion can be put together. Each cancer cell, over the course of time, will diffuse to the left or right by a single step. Due to diffusion, each cancer cells in time t will move either one step to the left or one step to the right (i.e., $\pm \delta x$). Due to advection, each cancer cells will also move ($u \delta t$) in the cross-flow direction as shown in Figure 2. The crossflow does not affect whether or not cancer cells diffuse to the right or left; rather, its presence only amplifies the effect of the original process.

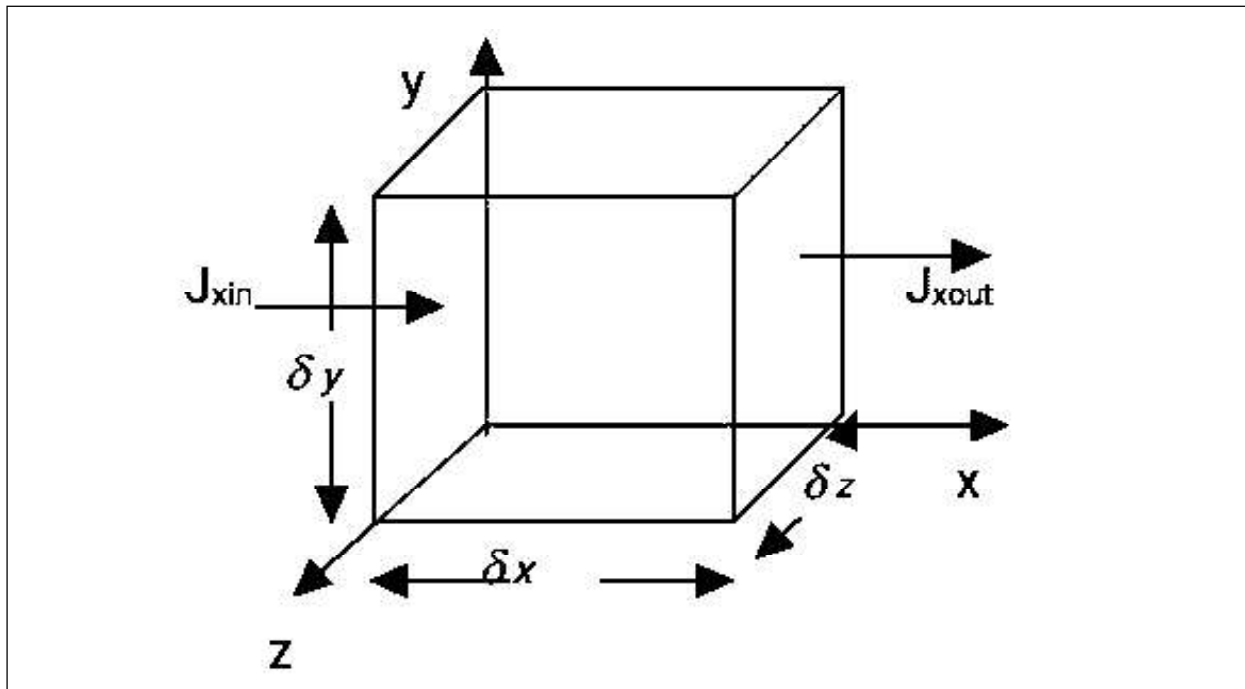


Figure 2: Schematic Diagram of a Control Volume with Cross Flow

3.1. Methods of Solution

The Finite Difference Technique was used for this research. Cahn-Hilliard, diffusion, and concentration equations are solved by means of two numerical schemes: a central Crank-Nicolson scheme and a central Difference scheme. By discretizing the supplied equation and developing numerical techniques analogous to the equations, the approaches obtain a finite system of linear or nonlinear algebraic equations from the Partial Differential Equations. The discretized equations were solved in MATLAB using the boundary conditions obtained.

3.1.1. Central Difference Scheme

The Central Difference scheme is a finite difference method used to get numerical solutions to a differential equation in applied mathematics by optimizing the approximation for the differential operator at the center of the patch under discussion. Its benefits include a quicker convergence rate than other finite differencing methods like the forward and backward differencing methods, as well as being straightforward to comprehend and apply at least for simple material relations.

3.1.2. Crank Nicolson Scheme

In a central Crank Nicolson scheme, the temporal variable t is replaced by forward difference scheme; y is replaced by central difference scheme while x is by the average of central difference approximation at j^{th} and $(j + 1)^{th}$ level.

3.2. Dimensionalizing Tumor Concentration Equation

The focus is to solve the concentration equation for Tumor concentration $C(x,y,t)$. In dimensionless variables, the governing equation is:

$$\frac{\partial C}{\partial t} + u \frac{\partial C}{\partial x} + v \frac{\partial C}{\partial y} = \frac{1}{Pe} \left(\frac{\partial^2 C}{\partial x^2} + \frac{\partial^2 C}{\partial y^2} \right) \tag{3.1}$$

where $u(x, y, t)$ and $v(x, y, t)$ are the given divergence-free advective velocity vector fields along x and y directions respectively, t is time and $C(x, y, t)$ is the Tumor concentration levels in human body tissues.

$$Pe = \frac{UL}{D} \tag{3.2}$$

Pe is the Peclet number, where U is an axial velocity, L is arterial length, and D is the diffusivity of the Tumor cells.

Substituting Equation (3.2) into Equation (3.1) gives

$$\frac{\partial C}{\partial t} + u \frac{\partial C}{\partial x} + v \frac{\partial C}{\partial y} = Pe \left(\frac{\partial^2 C}{\partial x^2} + \frac{\partial^2 C}{\partial y^2} \right) \quad \dots(3.3)$$

3.3. Discretization of Concentration Equation

The partial differential equation for concentration was discretized to form a central Crank Nicolson scheme which was eventually solved using the finite difference method. In application, Equation (3.3) is discretized to study the effects of Peclet number for Tumor concentration levels. Using a central difference numerical scheme, C_t is replaced by forward difference scheme while C_{xx} is the average of central difference approximation at j^{th} and $j+1^{\text{th}}$ level, and C_{yy} is replaced by central difference approximation. When these approximations are substituted into Equation (3.3), and taking $u=v=1$, the second derivative in concentration equation at node could be represented as follows:

$$\frac{C_{i,j}^{n+1} - C_{i,j}^n}{\Delta t} + \frac{C_{i+1,j}^n - C_{i-1,j}^n}{2\Delta x} + \frac{C_{i,j+1}^n - C_{i,j-1}^n}{2\Delta y} = Pe \left[\frac{1}{2} \left(\frac{C_{i+1,j}^n - 2C_{i,j}^n + C_{i-1,j}^n}{(\Delta x)^2} + \frac{C_{i,j+1}^n - 2C_{i,j}^n + C_{i,j-1}^n}{(\Delta y)^2} \right) + \frac{C_{i,j+1}^n - 2C_{i,j}^n + C_{i,j-1}^n}{(\Delta y)^2} \right] \quad \dots(3.4)$$

The effect of Pe number was investigated on the Tumor concentration levels. Taking $\phi = \frac{\Delta t}{(\Delta x)} = \frac{\Delta t}{(\Delta y)}$, and

$\mu = \frac{\Delta t}{(\Delta x)^2} = \frac{\Delta t}{(\Delta y)^2}$, $\Delta x = \Delta y$ and multiply by $2\Delta t$ throughout Equation (3.4) and re-arranging, we get the scheme below is obtained:

$$(\phi - \mu Pe)C_{i+1,j}^n - (\phi + \mu Pe)C_{i-1,j}^n + (6\mu Pe - 2)C_{i,j}^n = -\phi C_{i,j+1}^n + \mu Pe C_{i-1,j+1}^n + (2\mu Pe + \phi)C_{i,j-1}^n + \mu Pe C_{i+1,j+1}^n - 2C_{i,j}^{n+1} \quad \dots(3.5)$$

Taking $\Delta x = \Delta y = 0.1$, and $\Delta t = 0.01$, $\Rightarrow \phi = 0.1$ and $\mu = 2$ results to central difference scheme below:

$$(0.1 - 2Pe)C_{i+1,j}^n - (0.1 - 2Pe)C_{i-1,j}^n + (12Pe - 2)C_{i,j}^n = -0.1C_{i,j+1}^n + 2PeC_{i-1,j+1}^n + (4Pe + 0.1)C_{i,j-1}^n + 2PeC_{i+1,j+1}^n - 2C_{i,j}^{n+1} \quad \dots(3.6)$$

The above central difference scheme can be in form of 6 algebraic equations when $i = 1, 2, \dots, 6$ with $j = 1$ and $n = 0$ as:

$$\left. \begin{aligned} (0.1 - 2Pe)C_{2,1}^0 - (0.1 - 2Pe)C_{0,1}^0 + (12Pe - 2)C_{1,1}^0 &= -0.1C_{1,2}^0 + 2PeC_{0,2}^0 + (4Pe + 0.1)C_{1,0}^0 + 2PeC_{2,2}^0 - 2C_{1,1}^1 \\ (0.1 - 2Pe)C_{3,1}^0 - (0.1 - 2Pe)C_{1,1}^0 + (12Pe - 2)C_{2,1}^0 &= -0.1C_{2,2}^0 + 2PeC_{1,2}^0 + (4Pe + 0.1)C_{2,0}^0 + 2PeC_{3,2}^0 - 2C_{2,1}^1 \\ (0.1 - 2Pe)C_{4,1}^0 - (0.1 - 2Pe)C_{2,1}^0 + (12Pe - 2)C_{3,1}^0 &= -0.1C_{3,2}^0 + 2PeC_{2,2}^0 + (4Pe + 0.1)C_{3,0}^0 + 2PeC_{4,2}^0 - 2C_{3,1}^1 \\ (0.1 - 2Pe)C_{5,1}^0 - (0.1 - 2Pe)C_{3,1}^0 + (12Pe - 2)C_{4,1}^0 &= -0.1C_{4,2}^0 + 2PeC_{3,2}^0 + (4Pe + 0.1)C_{4,0}^0 + 2PeC_{5,2}^0 - 2C_{4,1}^1 \\ (0.1 - 2Pe)C_{6,1}^0 - (0.1 - 2Pe)C_{4,1}^0 + (12Pe - 2)C_{5,1}^0 &= -0.1C_{5,2}^0 + 2PeC_{4,2}^0 + (4Pe + 0.1)C_{5,0}^0 + 2PeC_{6,2}^0 - 2C_{5,1}^1 \end{aligned} \right\} \quad \dots(3.7)$$

the following initial and boundary conditions were applied to Equation (3.7)

$$C(x, y, 1) = 0, t = 0 \quad \dots(3.8)$$

$$C(0, y, t) = 10, C(x, 0, t) = C(x, 2, t) = 0, t > 0, x \neq y \quad \dots(3.9)$$

The above algebraic equations in (3.7) can be written in matrix form as:

$$\begin{bmatrix} (12Pe - 2) & (0.1 - 2Pe) & 0 & 0 & 0 & 0 \\ -(0.1 + 2Pe) & (12Pe - 2) & (0.1 - 2Pe) & 0 & 0 & 0 \\ 0 & -(0.1 + 2Pe) & (12Pe - 2) & (0.1 - 2Pe) & 0 & 0 \\ 0 & 0 & -(0.1 + 2Pe) & (12Pe - 2) & (0.1 - 2Pe) & 0 \\ 0 & 0 & 0 & -(0.1 + 2Pe) & (12Pe - 2) & (0.1 - 2Pe) \\ 0 & 0 & 0 & 0 & -(0.1 + 2Pe) & (12Pe - 2) \end{bmatrix} \begin{bmatrix} C_{1,1}^0 \\ C_{2,1}^0 \\ C_{3,1}^0 \\ C_{4,1}^0 \\ C_{5,1}^0 \end{bmatrix} = \begin{bmatrix} 1 + 40Pe \\ 20Pe \\ 20Pe \\ 20Pe \\ 20Pe \end{bmatrix} \quad \dots(3.10)$$

Solving the matrix system Equation (3.10) using *MATLAB*, solutions were obtained for varying values of *Pe*. The results were provided in Table 3.

3.4. Discretization of Cahn-Hilliard Model

Equation (3.10) was discretized to study the effects of mobility *M*, and density δ , of Tumor cells. Using a central difference numerical scheme, ϕ_{xx} was replaced by forward difference scheme. ϕ_{xx} was considered the average of central difference approximation at j^{th} and $j+1^{th}$ level, and ϕ_{yy} was replaced by central difference approximation. These approximations were substituted into Equation (3.11). Letting the superscript *n* indicate the time (temporal variable) while the subscript *i* and *j* indicate the spatial variable *x* and *y*, discretization of Equation (2.10) gives:

$$\begin{aligned} \frac{\phi_{i,j}^{n+1} - \phi_{i,j}^n}{\Delta t} = M\rho \left(\frac{1}{2} \left(\frac{(\phi_{i+1,j}^n - 2\phi_{i,j}^n + \phi_{i-1,j}^n)}{(\Delta x)^2} + \frac{\phi_{i+1,j+1}^n - 2\phi_{i,j+1}^n + \phi_{i-1,j+1}^n}{(\Delta x)^2} \right) + \frac{\phi_{i,j+1}^n - 2\phi_{i,j}^n + \phi_{i,j-1}^n}{(\Delta y)^2} \right) \\ - v \left(\frac{\phi_{i+1,j}^n - \phi_{i-1,j}^n}{(2\Delta x)} + \frac{\phi_{i,j+1}^n - \phi_{i,j-1}^n}{(2\Delta y)} \right) + \frac{\phi_{i+1,j}^n + \phi_{i,j}^n}{2} S_T \end{aligned} \quad \dots(3.11)$$

Similarly, in three dimension the subscript *i* and *k* indicate the spatial variable *x* and *z*.

$$\begin{aligned} \frac{\phi_{i,k}^{n+1} - \phi_{i,k}^n}{\Delta t} = M\rho \left(\frac{1}{2} \left(\frac{(\phi_{i+1,k}^n - 2\phi_{i,k}^n + \phi_{i-1,k}^n)}{(\Delta x)^2} + \frac{\phi_{i+1,k+1}^n - 2\phi_{i,k+1}^n + \phi_{i-1,k+1}^n}{(\Delta x)^2} \right) + \frac{\phi_{i,k+1}^n - 2\phi_{i,k}^n + \phi_{i,k-1}^n}{(\Delta y)^2} \right) \\ - v \left(\frac{\phi_{i+1,k}^n - \phi_{i-1,k}^n}{(2\Delta x)} + \frac{\phi_{i,k+1}^n - \phi_{i,k-1}^n}{(2\Delta y)} \right) + \frac{\phi_{i+1,k}^n + \phi_{i,k}^n}{2} S_T \end{aligned} \quad \dots(3.12)$$

Taking constant values of *v* and S_T so that $v = S_T = 1$ and multiplying by $2 \Delta t$ with square mesh for variables $\Delta x = \Delta y$ yields

$$\begin{aligned} \phi_{i,j}^{n+1} - \phi_{i,j}^n = \frac{M\rho\Delta t}{(\Delta x)^2} (\phi_{i+1,j}^n - 2\phi_{i,j}^n + \phi_{i-1,j}^n - \phi_{i+1,j+1}^n - 2\phi_{i,j+1}^n + \phi_{i-1,j+1}^n + 2\phi_{i,j+1}^n - 4\phi_{i,j}^n + 2\phi_{i,j-1}^n) \\ - \frac{\Delta t}{\Delta x} (\phi_{i+1,j}^n - \phi_{i-1,j}^n + \phi_{i,j+1}^n - \phi_{i,j-1}^n) + \Delta t (\phi_{i+1,j}^n + \phi_{i,j}^n) \end{aligned} \quad \dots(3.13)$$

Taking the mesh sizes $r = \frac{\Delta t}{(\Delta x)^2}$, $\tau = \frac{\Delta t}{\Delta x}$, $\xi = \Delta t$

$$\begin{aligned} \phi_{i,j}^{n+1} - \phi_{i,j}^n = M\rho r (\phi_{i+1,j}^n - 2\phi_{i,j}^n + \phi_{i-1,j}^n - \phi_{i+1,j+1}^n - 2\phi_{i,j+1}^n + \phi_{i-1,j+1}^n + 2\phi_{i,j+1}^n - 4\phi_{i,j}^n + 2\phi_{i,j-1}^n) \\ - \tau (\phi_{i+1,j}^n - \phi_{i-1,j}^n + \phi_{i,j+1}^n - \phi_{i,j-1}^n) + \xi (\phi_{i+1,j}^n + \phi_{i,j}^n) \end{aligned} \quad \dots(3.14)$$

But if $\Delta t = 0.01$, $\Delta x = 0.1$, $r = \frac{0.01}{(0.1)^2} = 1$, $\tau = \frac{0.01}{0.1} = 0.1$, $\xi = \frac{0.01}{1} = 0.01$

Equation (3.14) becomes

$$\begin{aligned} \phi_{i,j}^{n+1} - \phi_{i,j}^n = M\rho (\phi_{i+1,j}^n - 2\phi_{i,j}^n + \phi_{i-1,j}^n + \phi_{i+1,j+1}^n - 2\phi_{i,j+1}^n + \phi_{i-1,j+1}^n + 2\phi_{i,j+1}^n - 4\phi_{i,j}^n + 2\phi_{i,j-1}^n) \\ - 0.1 (\phi_{i+1,j}^n - \phi_{i-1,j}^n + \phi_{i,j+1}^n - \phi_{i,j-1}^n) + 0.01 (\phi_{i+1,j}^n + \phi_{i,j}^n) \end{aligned} \quad \dots(3.15)$$

multiplying both sides of Equation (3.15) by 100 gives

$$\begin{aligned} 100\phi_{i,j}^{n+1} - 100\phi_{i,j}^n = 100M\rho (\phi_{i+1,j}^n - 2\phi_{i,j}^n + \phi_{i-1,j}^n + \phi_{i+1,j+1}^n - 2\phi_{i,j+1}^n - \phi_{i-1,j+1}^n + 2\phi_{i,j+1}^n - 4\phi_{i,j}^n + 2\phi_{i,j-1}^n) \\ + 100\phi_{i+1,j}^n - 100\phi_{i-1,j}^n + 100\phi_{i,j+1}^n - 100\phi_{i,j-1}^n + \phi_{i+1,j}^n + \phi_{i,j}^n \end{aligned} \quad \dots(3.16)$$

Putting the $j + 1$ level on LHS of Equation (3.16) yields

$$\begin{aligned}
 -20M\rho\phi_{i+1,j+1}^n + (1 - 50M\rho)\phi_{i,j+1}^n - 20M\rho\phi_{i-1,j+1}^n &= (10.01 - 40M\rho)\phi_{i,j}^n \\
 + (10M\rho - 0.99)\phi_{i+1,j}^n + (10M\rho + 1)\phi_{i-1,j}^n + (10M\rho + 1)\phi_{i,j-1}^n - 10\phi_{i,j}^{n+1} &\dots(3.17)
 \end{aligned}$$

Taking $i=1, 2, 3, 4, 5, \dots, n=0, j=1$, gives the algebraic equations

$$\begin{aligned}
 -20M\rho\phi_{2,2}^0 + (1 - 50M\rho)\phi_{1,2}^0 - 20M\rho\phi_{0,2}^0 &= (10M\rho - 0.99)\phi_{2,1}^0 + (10.01 - 40M\rho)\phi_{1,1}^0 + (10M\rho + 1)\phi_{0,1}^0 + (10M\rho + 1)\phi_{1,0}^0 - 10\phi_{1,1}^1 \\
 -20M\rho\phi_{3,2}^0 + (1 - 50M\rho)\phi_{2,2}^0 - 20M\rho\phi_{1,2}^0 &= (10M\rho - 0.99)\phi_{3,1}^0 + (10.01 - 40M\rho)\phi_{2,1}^0 + (10M\rho + 1)\phi_{1,1}^0 + (10M\rho + 1)\phi_{2,0}^0 - 10\phi_{2,1}^1 \\
 -20M\rho\phi_{4,2}^0 + (1 - 50M\rho)\phi_{3,2}^0 - 20M\rho\phi_{2,2}^0 &= (10M\rho - 0.99)\phi_{4,1}^0 + (10.01 - 40M\rho)\phi_{3,1}^0 + (10M\rho + 1)\phi_{2,1}^0 + (10M\rho + 1)\phi_{3,0}^0 - 10\phi_{3,1}^1 \\
 -20M\rho\phi_{5,2}^0 + (1 - 50M\rho)\phi_{4,2}^0 - 20M\rho\phi_{3,2}^0 &= (10M\rho - 0.99)\phi_{5,1}^0 + (10.01 - 40M\rho)\phi_{4,1}^0 + (10M\rho + 1)\phi_{3,1}^0 + (10M\rho + 1)\phi_{4,0}^0 - 10\phi_{4,1}^1 \\
 -20M\rho\phi_{6,2}^0 + (1 - 50M\rho)\phi_{5,2}^0 - 20M\rho\phi_{4,2}^0 &= (10M\rho - 0.99)\phi_{6,1}^0 + (10.01 - 40M\rho)\phi_{5,1}^0 + (10M\rho + 1)\phi_{4,1}^0 + (10M\rho + 1)\phi_{5,0}^0 - 10\phi_{5,1}^1
 \end{aligned}
 \dots(3.18)$$

Taking the initial $\phi(x, y, 0) = \phi(x, 1, 0) = 1$, and boundary conditions, $\phi(0, y, t) = \phi(x, 0, t) = 1$, the above system of algebraic equation become

$$\begin{bmatrix} (-50M\rho) & -20M\rho & 0 & 0 & 0 \\ -20M\rho & (-50M\rho) & -20M\rho & 0 & 0 \\ 0 & -20M\rho & (-50M\rho) & -20M\rho & 0 \\ 0 & 0 & -20M\rho & (-50M\rho) & -20M\rho \\ 0 & 0 & 0 & -20M\rho & (-50M\rho) \end{bmatrix} \begin{bmatrix} \phi_{1,2}^0 \\ \phi_{2,2}^0 \\ \phi_{3,2}^0 \\ \phi_{4,2}^0 \\ \phi_{5,2}^0 \end{bmatrix} = \begin{bmatrix} 10M\rho - 0.98 \\ -10M\rho + 1.02 \\ -10M\rho + 1.02 \\ -10M\rho + 1.02 \\ -10M\rho + 1.02 \end{bmatrix} \dots(3.19)$$

3.5. Reaction-Diffusion Equation

The Cahn-Hilliard model (Uthamacumaran, 2020) was used as a more involving reaction-diffusion model. The model emphasizes the mutually beneficial relationships between ECM and cancer Tumor and metastatic capacities of cancer cells. More elaborate extensions of the model were explored and its various forms, including additional terms related to Tumor cell proliferation, ECM renewal, and alternative functions representing Tumor cell MDE generation. This study focused to uncover how cancer cells are able to create and secrete the MDE, which in turn degrades the ECM and initiates migration of the cells towards healthy regions of the tissue. The model was given as:

$$\frac{\partial u}{\partial t} = D \left(\frac{\partial^2 u}{\partial x^2} + \frac{\partial^2 u}{\partial y^2} \right) + \alpha u - \beta u \dots(3.20)$$

3.6. Discretization of Reaction-Diffusion Equation

For simplicity let $D = 1$

$$\frac{M_{i,j}^{n+1} - M_{i,j}^n}{\Delta t} = \frac{M_{i+1,j}^n - 2M_{i,j}^n + M_{i-1,j}^n}{(\Delta x)^2} + \frac{M_{i,j+1}^n - 2M_{i,j}^n + M_{i,j-1}^n}{(\Delta y)^2} (\alpha - \beta) M_{i,j}^n \dots(3.21)$$

Multiply by Δt let $\Delta x = \Delta y$, $\frac{\Delta t}{\Delta x} = \frac{0.01}{0.1} = \frac{1}{10}$, $\frac{\Delta t}{(\Delta x)^2} = \frac{0.01}{(0.1)^2} = \frac{1}{100} = 0.01$

$$M_{i,j+1}^n - M_{i,j}^n = 0.01M_{i+1,j}^n - 0.02M_{i,j}^n + 0.01M_{i-1,j}^n + 0.01M_{i,j+1}^n - 0.02M_{i,j}^n + 0.01M_{i,j-1}^n + 0.01(\alpha - \beta)M_{i,j}^n \dots(3.22)$$

and

$$0.01M_{i+1,j}^n + (1 - 0.04 + \alpha - \beta)M_{i,j}^n + 0.01M_{i-1,j}^n = (1 - 0.01)M_{i,j+1}^n - 0.01M_{i,j-1}^n \dots(3.23)$$

Simplifying Equation (3.23) gives

$$0.01M_{i+1,j}^n + (0.96 + \alpha - \beta)M_{i,j}^n + 0.01M_{i-1,j}^n = 0.99M_{i,j+1}^n - 0.01M_{i,j-1}^n \dots(3.24)$$

In order to solve the system Equation (3.24), initial conditions are applied resulting to the algebraic equations (3.25) below:

$$\begin{aligned}
 0.01M_{2,1}^0 + (0.96 + \alpha - \beta)M_{1,1}^0 + 0.01M_{0,1}^0 &= 0.99MM_{1,2}^0 - 0.01M_{1,0}^0 \\
 0.01M_{3,1}^0 + (0.96 + \alpha - \beta)M_{2,1}^0 + 0.01M_{1,1}^0 &= 0.99MM_{2,2}^0 - 0.01M_{2,0}^0 \\
 0.01M_{4,1}^0 + (0.96 + \alpha - \beta)M_{3,1}^0 + 0.01M_{2,1}^0 &= 0.99MM_{3,2}^0 - 0.01M_{3,0}^0 \\
 0.01M_{5,1}^0 + (0.96 + \alpha - \beta)M_{4,1}^0 + 0.01M_{3,1}^0 &= 0.99MM_{4,2}^0 - 0.01M_{4,0}^0 \\
 0.01M_{6,1}^0 + (0.96 + \alpha - \beta)M_{5,1}^0 + 0.01M_{4,1}^0 &= 0.99MM_{5,2}^0 - 0.01M_{5,0}^0
 \end{aligned}
 \tag{3.25}$$

Taking the initial $M(x, y, 0) = 10$ and boundary conditions, $M(x, 0, 0) = 10$, the above system of algebraic equation (3.25) becomes:

$$\begin{bmatrix}
 (0.96 + \alpha - \beta) & 0.01 & 0 & 0 & 0 \\
 0.01 & (0.96 + \alpha - \beta) & 0.01 & 0 & 0 \\
 0 & 0.01 & (0.96 + \alpha - \beta) & 0.01 & 0 \\
 0 & 0 & 0.01 & (0.96 + \alpha - \beta) & 0.01 \\
 0 & 0 & 0 & 0.01 & (0.96 + \alpha - \beta)
 \end{bmatrix}
 \begin{bmatrix}
 M_{1,1}^0 \\
 M_{2,1}^0 \\
 M_{3,1}^0 \\
 M_{4,1}^0 \\
 M_{5,1}^0
 \end{bmatrix}
 =
 \begin{bmatrix}
 8.895 \\
 9.895 \\
 9.895 \\
 9.895 \\
 9.895
 \end{bmatrix}
 \tag{3.26}$$

4. Results and Discussion

The simulation results given focus on the effects of the mobility, M , Tumor density, ρ , and Peclet number, Pe , Extracellular Matrix, α and Matrix degradation Enzymes, β on Tumor growth rate, Tumor cells concentration and Tumor invasion respectively.

4.1. Effects of Cell Density on Tumor Growth Rate

Equation (3.26) was solved in MATLAB to obtain the results of the effects of ρ on Tumor growth rate when M held constant. The results were recorded as shown in Table 1.

Tumour Density	Length of Tumour Spread from Source				
	0	1	2	3	4
$\rho = 3000\text{kg/m}^3$	3.62859E20	5.664E14	1.283E13	3.333E19	-0.9283E20
$\rho = 2000\text{kg/m}^3$	5.30254E20	5.4666E19	4.81279E19	7.99666E19	-0.7266E20
$\rho = 1000\text{kg/m}^3$	6.04611E20	1.6999E20	9.31538E19	1.33999E20	-0.6016E20

The above results were presented in Figure 3.

Figure 3 shows how Tumor density impacts Tumor growth. Figure 3 shows that Tumor growth slows with increasing Tumor density and accelerates in the opposite direction as Tumors spread from their original location. Tumors formed in high-density cells are suppressed through the application of compressive pressures, leading to smaller Tumors than those grown in low-density cells. As a result, an increase in cell density typically results in a smaller Tumor.

4.2. Effects of Mobility on Tumor Growth Rate

Equation (3.26) was solved in MATLAB and obtain the results of the effects of M on Tumor growth rate as shown in Table 2.

The above results were presented in Figure 4.

Figure 4 shows how the movement of cancer cells affects the formation of Tumors. Tumor growth rates are observed to rise alongside cell motility. As mobility decreases, the distance a Tumor can travel from its initial site increases. Tumor and normal host cell motility play a role in Tumor metastasis at multiple stages, including Tumor cell motility during

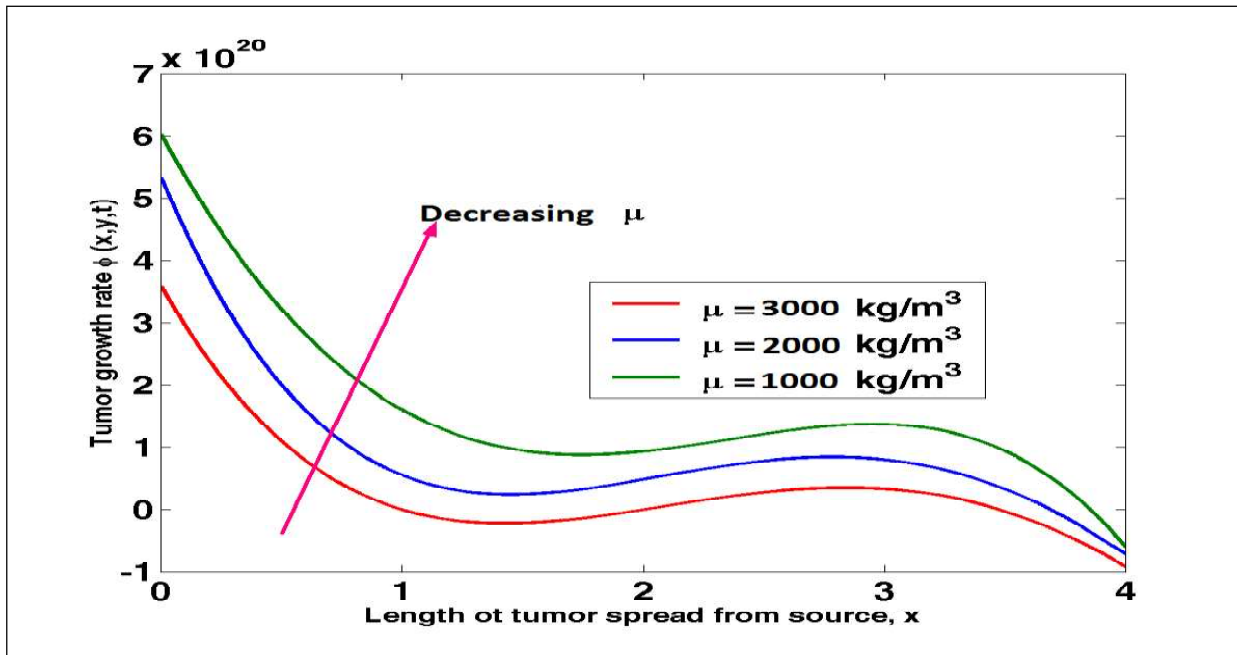


Figure 3: Graph of Tumor Growth Rate Against Length of Tumor Spread from Source at Varying Tumor Density

Table 2: Value of Tumor Growth Rates for Mobility

Mobility	Length of Tumor Spread from Source				
	0	1	2	3	4
M = 10	2.2815E20	6.664E14	1.283E13	1.333*10 ⁸	1.2283E6
M = 20	4.32E20	1.499E15	2.88E13	1.9999E8	1.9236E6
M = 30	1.025E21	2.666E15	5.127E13	2.6663E8	2.5646E6

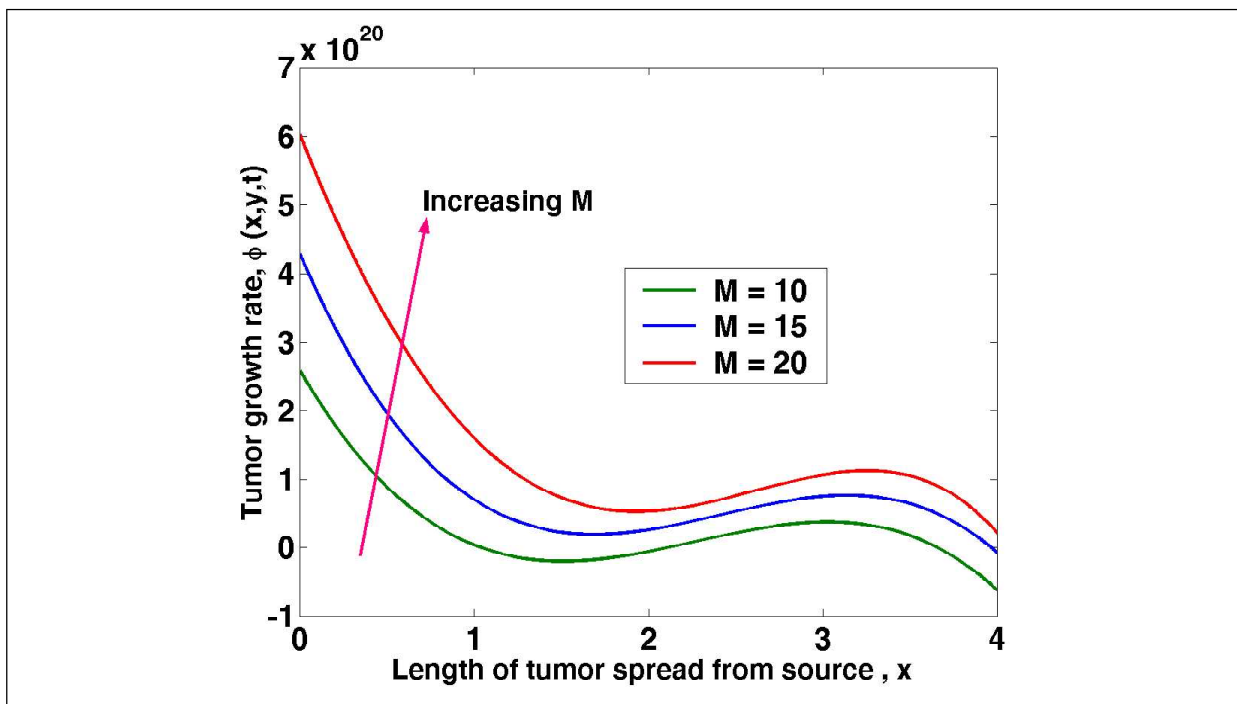


Figure 4: Tumor Growth Rate Against Length of Tumor Spread from Source at Varying Mobility

basement membrane breakdown, Tumor cell motility during escape from the primary Tumor, Tumor cell motility during migration to blood and lymphatic vessels, and Tumor cell motility during intravasation, extravasation, and metastasis to distant organs.

4.3. Effects of P'eclet Number on Tumor Concentration

Equation (3.26) was solved in MATLAB to obtain the results of the effects of Peclet number on Tumor concentration as shown in Table 3.

Table 3: Value of Tumor Concentration for Various P'eclet Number					
Peclet Number	Length of Tumour Spread from Source				
	0	1	2	3	4
Pe = 2.0	17.4916	21.75409	20.65741	14.59695	6.397966
Pe = 2.3	17.37959	21.11846	20.08196	14.51852	6.699591
Pe = 2.5	20.42459	27.20341	27.65395	21.47235	10.92022

The above results are presented in Figure 5.

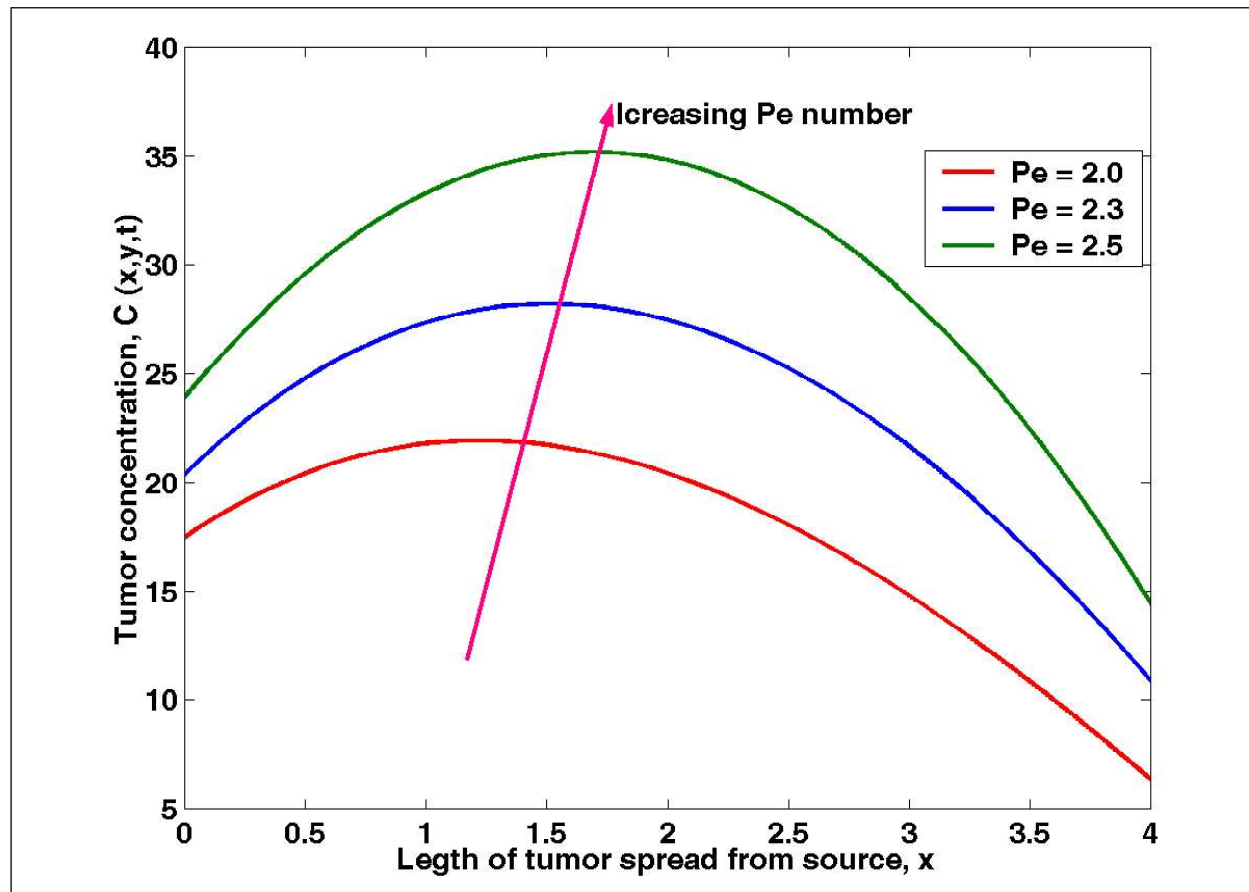


Figure 5: Tumor Concentration Against Length of Tumor Spread from Source at Varying P'eclet Number

The effect of Peclet number on Tumor concentration can be observed from figure 6. Initially, an increase in Peclet number leads to increases in the Tumor growth rate. The effect of Pe on concentration is seen to have been very significant in two-phase flows in Tumor cells. From the first phase, it is clearly seen that, with increasing values of Pe, the peak of Tumor concentration increases from 0 to 1.5 and the profile of concentration becomes flatter. The peak values of Tumor concentration are 1.5 to 2.0. With increasing values of Pe beyond 2.0, the initial Tumor cells concentration decreases for a fixed radius from 2.0 to 4.0. From Figure 5 it is worth noting that the Pe governs the initial concentration of Tumor cells in the human body system. For this reason, the concentration of the Tumor cells reduces for higher

values of Pe . The peak of the mean concentration decreases with the increase in the value of Pe and this effect is very significant in small cell radius. This study may be applied for investigation of the transportation process of drugs or plasma proteins in blood flow through small arteries.

4.4. Effects of ECM on Tumor Invasion

Equation (3.26) was solved in MATLAB and to obtain the results of the effects of ECM on Tumor invasion rate as shown in Table 4.

ECM Values	Length of Tumor Spread from Source				
	0	1	2	3	4
$\alpha_{ECM} = 0.01$	17.4916	21.75409	20.65741	14.59695	6.397966
$\alpha_{ECM} = 0.05$	17.37959	21.11846	20.08196	14.51852	6.699591
$\alpha_{ECM} = 0.10$	20.42459	27.20341	27.65395	21.47235	10.92022

The above results are presented in Figure 6.

Figure 6 displays the impact of extracellular matrix on Tumor invasion. Rise in ECM leads to decreases in the Tumor invasion rate. The ECM binds soluble substances, such as growth factors and other ECM-associated proteins. Skeletal muscle development from embryonic stage to senescence involves cell surface receptors interacting with ECM components and ECM-bound substances to regulate cell adhesion and cell signaling, consequently regulating activities as varied as proliferation, differentiation, migration, and apoptosis. Due to an increase in ECM in the cell milieu of aged muscle, satellite cells lose their capacity to differentiate into myogenic lineages. Collagen released by satellite cells can keep them dormant, and studies have shown that ECM protein components contribute to the myogenesis process of

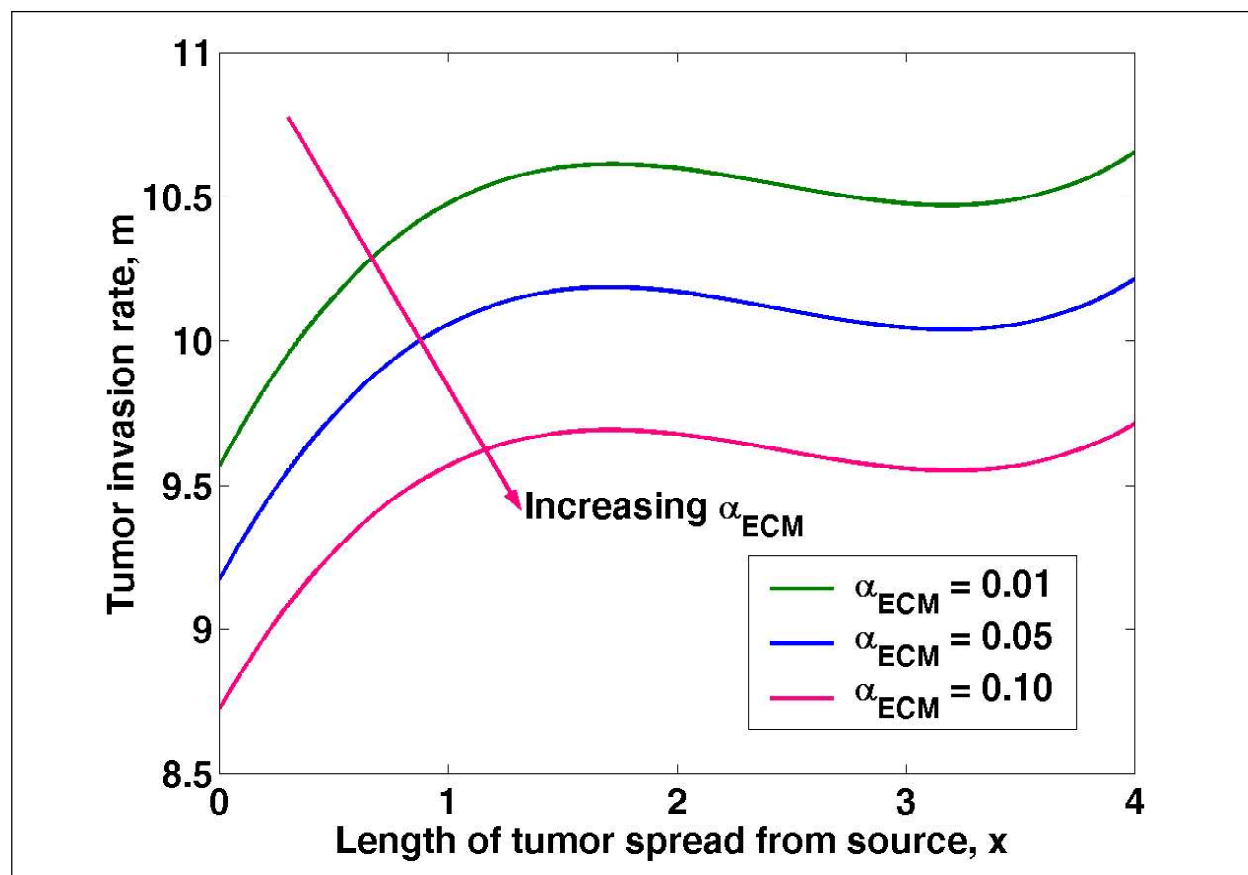


Figure 6: Tumor Invasion Against Length of Tumour Spread from Source at Varying ECM Number

skeletal muscle progenitor cells. Hence, it is safe to say that ECM plays a crucial role in preventing Tumor growth and sustaining normal cancer cell activity.

4.5. Effects of MDE on Tumor Invasion Rate

Equation (3.26) was solved in MATLAB and to obtain the results of the effects of MDE on Tumor invasion rate as shown in Table 5.

MDE Values	Length of Tumor Spread from Source				
	0	1	2	3	4
$\beta_{MDE} = 0.05$	17.4916	21.75409	20.65741	14.59695	6.397966
$\beta_{MDE} = 0.10$	17.37959	21.11846	20.08196	14.51852	6.699591
$\beta_{MDE} = 0.15$	20.42459	27.20341	27.65395	21.47235	10.92022

The above results are presented in Figure 7.

Figure 7 shows how MDE affects the pace of Tumor invasion. When DME levels rise, Tumors invade at a faster rate. During DME, the invading tissue’s extracellular matrix scaffolds are degraded in whole while a new, Tumor derived extracellular matrix is simultaneously formed to support the Tumor mass’s unchecked growth. As a result, it is safe to say that MDE plays a crucial role in promoting Tumor growth by degrading cancer cells’ physiological function and fostering the formation of skeletal muscle.

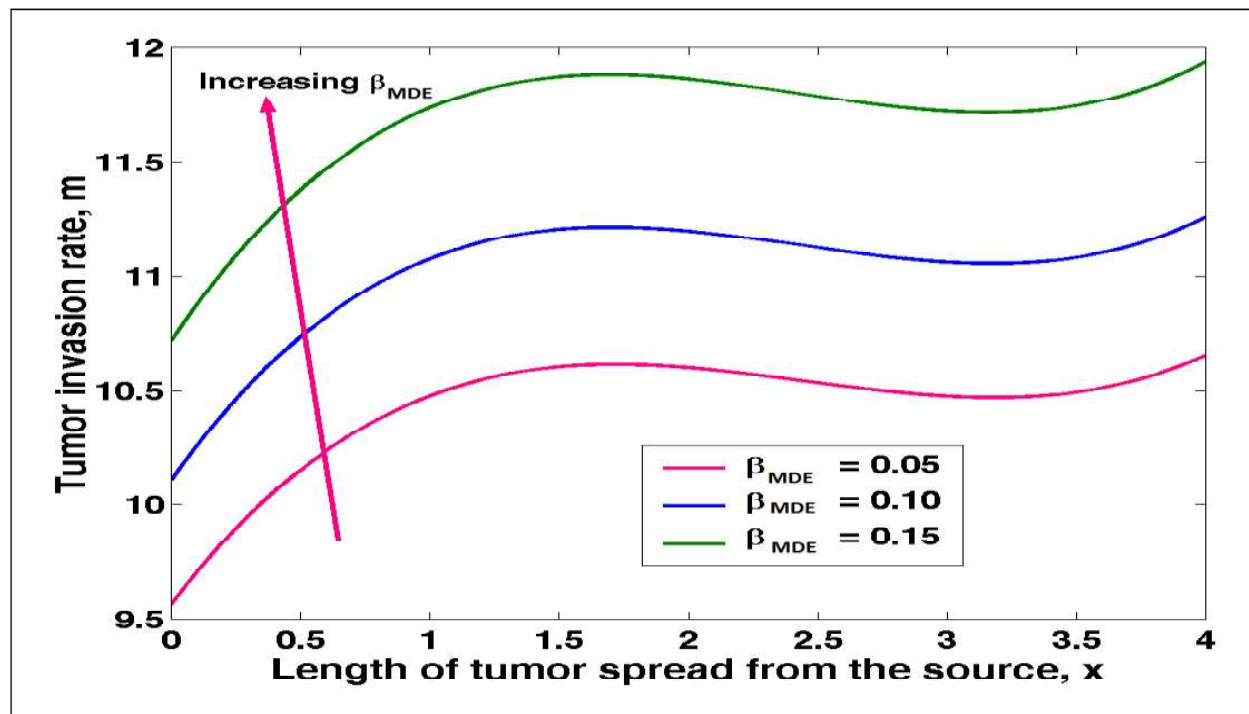


Figure 7: Tumor Invasion Rate Against Length of Tumor Spread from Source at Varying MDE

4.6. Equilibrium Point Between of ECM and MDEs in Tumor Invasion

Equation (3.26) was solved MATLAB and to obtain the results of the point of equilibrium between ECM = 0.05 and MDE = 0.05 on Tumor invasion rate as shown in Table 6.

The above results are presented in Figure 8.

Figure 8 demonstrates that the amount of extracellular matrix decreases with Tumor size and distance from the Tumor’s origin. This is because the cells are stuck together, whereas the graph of matrix degrading enzymes shows a

ECM and MDE Values	Length of Tumor Spread from Source				
	0	1	2	3	4
$\alpha_{ECM} = 0.05$	17.37959	21.11846	20.08196	14.51852	6.699591
$\beta_{MDE} = 0.05$	17.4916	21.75409	20.65741	14.59695	6.397966

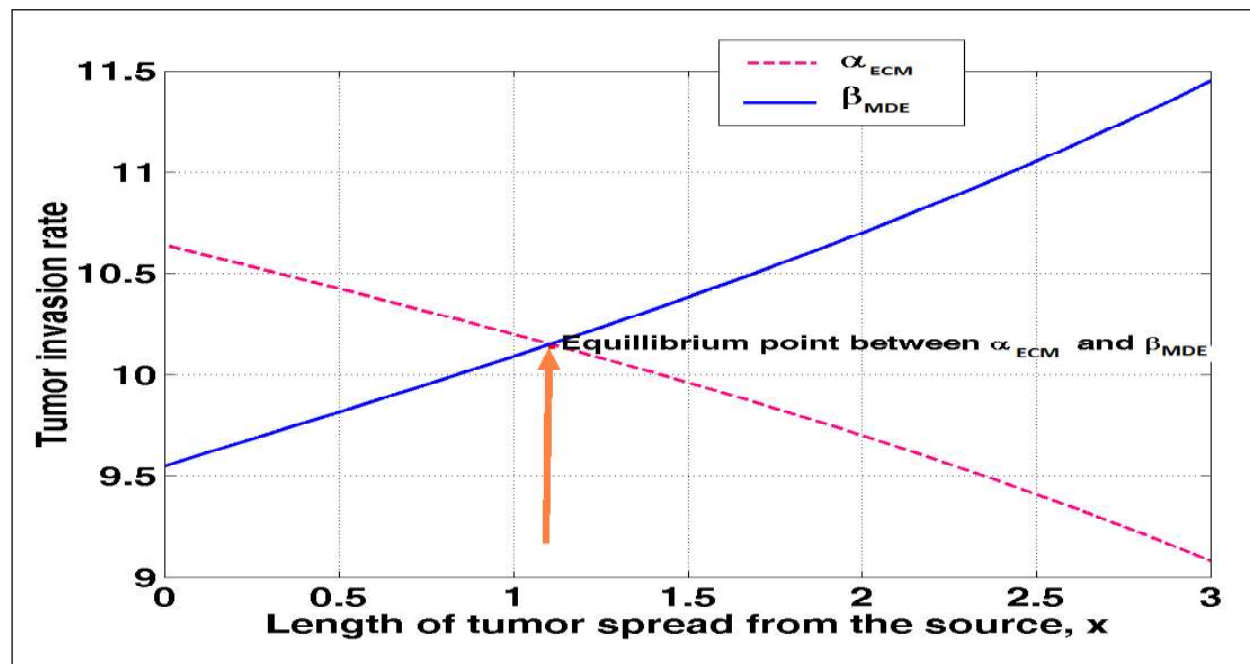


Figure 8: Tumor Invasion Rate Against Length of Tumor Spread from Source at Equilibrium Point Between ECM and MDE

direct correlation between Tumor length and Tumor depth. Collagen, enzymes, and glycoproteins are just a few examples of the macromolecules and minerals that make up the extracellular matrix, which provides structural and biochemical support to the cells in their immediate vicinity. The integrins on the cells of the tissues it is connecting are the point of attachment for the extracellular matrix. Proteins known as integrins bind to the cytoskeleton of cells. Molecules of this kind are exudates from neighbouring cells. Yet, Tumor cells’ own matrix degrading enzymes (MDEs) break down the extracellular matrix, freeing cancer cells to spread across the body. As the point where the ECM and the MDEs meet, equilibrium is established.

5. Summary and Conclusion

A numerical study was performed to analyze the effects of the mobility M , Tumor density, μ and Peclet number, Pe , Extracellular Matrix, α and Matrix degradation Enzymes, β on Tumor growth rate Tumor cells concentration and Tumor invasion, respectively.

The following outcomes can be written from the study.

- An increase in the mobility leads to an increase in the Tumor growth rate.
- Surface heat transfer tends to decrease with an increase in Tumor growth rate.
- An increase in Peclet number leads to a decrease in Tumor concentration.
- An increase in ECM leads to an increase in Tumor growth rate.
- An increase in MDEs causes a decrease in Tumor growth rate.
- An increase in Peclet number leads to a decrease in Tumor growth rate.

6. Recommendations

From this study, the following areas arise for further analysis and development:

- An extension of this study to factor in a varying sources of Tumor, ST and dead cells, SD.
- An extension of this study to incorporate diffusion coefficient Tumor growth rate.

Acknowledgment

The authors acknowledge Kisii University (Department of Mathematics and Actuarial Sciences) for affiliation and support in academic resources.

References

- Akhtar, A., Majid, H., Abdul, G., Zafar, A., Kottakkaran, S., Alharthi, M. and Wasim, J. (2021). Numerical Simulations and Analysis for Mathematical Model of Avascular Tumor Growth Using Gompertz Growth Rate Function. Published by Elsevier BV. This is an open access article under the CC BY-NC-ND license (<http://creativecommons.org/licenses/by-nc-nd/4.0/>).
- Beerenwinkel, N., Roland, F., Schwarz, Gerstung, M. and Markowetz, F. (2015). Cancer Evolution: Mathematical Models and Computational Inference. *Systematic Biology*, 64(1), 2015, e25/<https://doi.org/10.1093/sysbio/syu081>
- Brassel, M. and Bretin, E. (2011). A Modified Phase Field Approximation for Mean Curvature Flow with Conservation of the Volume, *Math. Meth. Appl. Sci.*, 34(10), 1157-1180.
- Elaine, L. et al. (2009). Mathematical Oncology. Multiparameter Computational Modelling of Tumour Invasion. DOI: 10.1158/0008-5472.CAN-08-3438. Available online: www.aacrjournals.org
- Fornier, B., Laporte, D., Lebaudy, A., Sahin, A., Pinson, B., Ceschin, J. and Sagot, I. (2011). Metabolic status rather than cell cycle signals control quiescence entry and exit. *J Cell Biol.* Mar 21;192(6), 949-57. doi: 10.1083/jcb.201009028. Epub 2011 Mar 14. PMID: 21402786; PMCID: PMC3063145.
- Grego'rio, A., Fonseca, N., Moura, V., Lacierda, M., Figueredo, P., Simões, S. et al. (2016). Inoculated Cell Density as a Determinant Factor of the Growth Dynamics and Metastatic Efficiency of a Breast Cancer Murine Model. *PLoS ONE* 11(11), e0165817. Doi: 10.1371/journal.pone.0165817
- Gross, J.F. and Popel, A.S. (1979). Mathematical Models Of Transport Phenomena In Normal And Neoplastic Tissue, *Tumour Blood Circulation*, CRC Press, Peterson edition; (Google Scholar).
- Hasitha, N., Weerasinghe, Pamela, M., Burrage, [...]and Dan V., Nicolau. (2019). *Journal of Oncology*. Published online October, Doi: 10.1155/2019/2403483
- Johnson, K.E., Howard, M.W., Strasser, M.K., Lima, E.A.B.F., Huang, S. et al. (2019). Cancer Cell Population Growth Kinetics At Low Densities Deviate From the Exponential Growth Model and Suggest an Allee Effect. *PLoS Biol.*, 17(8): e3000399. <https://doi.org/10.1371/journal.pbio.3000399>
- Katira, P., Roger, T., Bonnacaze. and Muhammad, H. Zaman. (2013). Modelling the Mechanics Of Cancer: Effect Of Changes In Cellular And Extra-cellular Mechanical Properties. *Frontier in Oncology*, 11(3), 145. doi: 10.3389/fonc.2013.00145. PMID: 23781492; PMCID: PMC3678107.
- Kolev, M. and Zubik-Kowal, B. (2011). "Numerical Solutions for a Model of Tissue Invasion and Migration of Tumour Cells", *Computational and Mathematical Methods in Medicine*, Vol. 2011, Article ID 452320, 16 Pages, 2011. <https://doi.org/10.1155/2011/452320>
- Sharif, G.M. and Wellstein, A. (2015). Cell Density Regulates Cancer Metastasis via the Hippo Pathway. Doi: 10.2217/fon.15.268
- Socolofsky, S.A. and Jirka, G.H. (2002). *Environmental Fluid Mechanics. Part 1*, 2nd Edition, Institute for Hydrodynamics, University of Karlsruhe, Germany.
- Uthamacumaran, A. (2020). *Cancer: A Turbulence Problem*, 22(12), 759-769. Neoplasia, <https://doi.org/10.1016/j.neo.2020.09.008>.

- WHO. (2020). Global Cancer Observatory, [2020, December 18]. Cancer Data for Cancer Action. (<http://gco.iarc.fr/today/home>). GLOBOCAN_GCO [Twitter post] Retrieved from: <http://twitter.com/todayhome>
- Wise, S. M., Lowengrub, J. S., Frieboes, H. B. and Cristini, V. (2008). Three-dimensional multispecies nonlinear tumor growth—I: model and numerical method. *Journal of theoretical biology*, 253(3), 524-543.
- Xuelian, H., Zhang L. and Xuezhao, L. (2019). Toll-like Receptor 2 and Toll-like Receptor Regulation of Cancer Cell Stemness Mediated By Cell Death-induced High-mobility Group Box 1. *Biomedicine*, 40, 135-150.
- Zhang, X., Song, G., Liang, G. and Tian, T. (2022). Mathematical Modelling and Analysis of Tumour Chemotherapy. *Symmetry*, 14(4), 704, <https://doi.org/10.3390/sym14040704>

Appendix

Nomenclature

M , Mobility Parameter ($\text{m}^2/\text{V.s}$);
 N , Number of living cells per unit volume in Nanometers (nm);
 S_r , Net sources of tumour cells (nm);
 S_d , Net sources of dead cells (nm);
 μ , Density of the tumour ($\text{kg (m}^{-3}\text{)}$);
 $F(\varphi)$, Double well bulk energy (joule);
 ε , Parameter related to the thickness of the diffuse interface tumour and host domains;
 u , Tumor velocity(m/s);
 $\beta(t) \sqrt{F(\varphi)}$, Space–time dependent Lagrange multiplier;
 p , Pressure (N/m^2);
 n , Nutrient concentration;
 φ , Sum of the volume fractions of viable and dead tumour cells;
 ε , Host tissue;
 ψ , Dead tumour cells;
 P , Population density;
 P , Advection cancer invasion velocity;
 ν , Cancer cells diffusivity ($\mu\text{M}^2/\text{h}$);
 ρ , Density of a single tumour cell (kg.m^3);
 D_m , MDE diffusion coefficient;
 β , MDE production rate by cells;
 γ , MDE natural decay rate;
 $\Omega(t)$, Area occupied by tumour at time;
 C_p , Specific heat capacity ($\text{Jkg}^{-1}\text{k}^{-1}$);
 α , Repose angle;
 κ , Materials conductivity ($\text{Wm}^{-1}\text{k}^{-1}$);
 δ , Flowing layer depth; ,
 Pr ; Prandtl number; ,
 Pe , Peclet number; ,
 Re , Reynolds number;
 Sc , Schmidt number;
 J_x , Total flux of the cancer cells x-axis;
 J_y , Total flux of the cancer cells along the y-axis.